Supplement of Atmos. Chem. Phys., 25, 15197–15243, 2025
https://doi.org/10.5194/acp-25-15197-2025-supplement

Atmospheric Chemistry and Physics
Open Access
EGU

Supplement of

Quantifying European SF_6 emissions from 2005 to 2021 using a large inversion ensemble

Martin Vojta et al.

Correspondence to: Martin Vojta (martin.vojta@univie.ac.at)

S1 Measurements

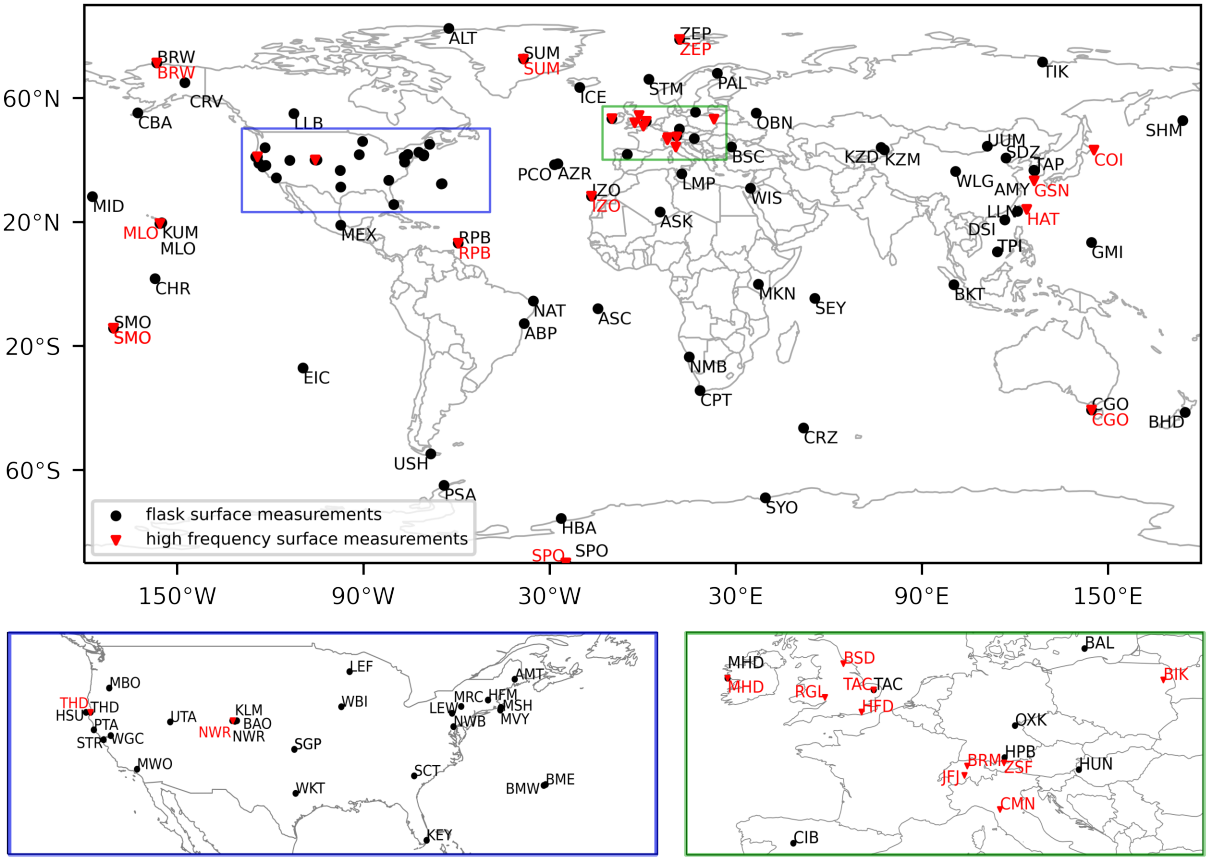

Figure S1. Locations of stations with continuous surface measurements (red triangles) and surface flask measurements (black dots) used in the inversion.

Table S1. Number of observations per year for the eight observation datasets used in the inversion.

Year	Global	Global excl. mountain	Global afternoon/night	Global high freq.	Europe	Europe excl. mountain	Europe afternoon/night	Europe high freq.
2005	31,653	23,454	15,111	22,414	16,248	11,363	11,255	6,999
2006	34,905	26,358	16,101	25,451	16,753	12,259	11,497	7,299
2007	37,561	29,391	18,299	26,086	18,796	14,787	13,529	7,319
2008	46,719	35,884	22,448	32,619	21,420	17,899	16,132	7,320
2009	46,948	35,488	24,302	30,589	21,754	18,240	17,983	5,395
2010	42,834	31,396	20,235	30,206	18,957	15,082	14,312	6,329
2011	56,633	42,425	29,247	36,500	30,023	23,749	22,586	9,890
2012	47,617	34,624	19,381	37,635	21,358	15,996	12,802	11,376
2013	48,633	38,185	21,477	36,143	22,563	19,985	14,958	10,073
2014	53,695	40,774	22,428	41,456	29,848	24,425	16,511	17,609
2015	50,232	37,383	20,648	39,396	26,365	20,761	14,715	15,529
2016	58,286	43,395	25,289	44,049	33,269	26,293	19,014	19,033
2017	55,213	43,334	25,408	39,817	34,096	27,073	20,125	18,700
2018	48,478	39,488	21,585	35,883	29,512	24,679	16,833	16,917
2019	44,958	37,561	17,129	37,066	27,006	22,193	12,660	19,114
2020	45,479	36,908	17,475	37,376	27,016	22,707	12,861	18,913
2021	36,102	28,408	14,303	29,100	17,825	14,361	9,738	10,823

Table S2. On-line surface stations monitoring SF_6 in and outside of Europe

Site ID	Station	Latitude	Longitude	Altitude[a]	Period
Europe					
BIK	Bialystok, Poland	53.2°N	23.0°E	180	2005-2008
BRM	Beromünster, Switzerland	47.2°N	8.2°E	797	2019-2020
BSD	Bilsdale, UK	54.4°N	1.1°W	379	2014-2020
CMN*	Monte Cimone, Italy	44.2°N	10.7°E	2172	2009-2017
HFD	Heathfield, UK	51.0°N	0.2°E	157	2014-2020
JFJ*	Jungfraujoch, Switzerland	46.5°N	8.0°E	3584	2005-2021
MHD	Mace Head, Ireland	53.3°N	9.9°W	26	2005-2021
RGL	Ridge Hill, UK	52.0°N	2.5°W	294	2012-2021
TAC	Tacolneston Tall Tower, UK	52.5°N	1.1°E	183	2012-2021
ZEP	Zeppelin, Ny-Alesund, Norway	78.9°N	11.9°E	490	2005-2021
ZSF*	Zugspitze-Schneefernerhaus, Germany	47.4°N	11.0°E	2670	2005-2021
Outside Europe					
BRW	Barrow, Alaska, USA	71.3°N	156.6°W	18	2005-2021
CGO	Cape Grim, Tasmania	40.7°S	144.7°E	164	2005-2021
COI	Cape Ochiishi, Japan	43.2°N	145.5°E	100	2011-2013
GSN	South Korea	33.3°N	126.2°E	89	2008-2021
HAT	Hateruma, Japan	24.1°N	123.8°E	47	2005-2019
IZO*	Izaña, Tenerife	28.3°N	16.5°W	2403	2007-2016
MLO*	Mauna Loa, Hawaii, USA	19.5°N	155.6°W	3407	2005-2021
NWR*	Niwot Ridge, Colorado, USA	40.0°N	105.5°W	3028	2005-2021
RPB	Ragged Point, Barbados	13.2°N	59.4°W	50	2005-2021
SMO	Cape Matatulu, American Samoa, USA	14.3°S	170.6°W	87	2005-2021
SPO	South Pole, Antarctica	90.0°S	24.8°W	2820	2005-2021
SUM	Summit, Greenland	72.6°N	38.5°W	3228	2007-2017
THD	Trinidad Head, USA	41.1°N	124.2°W	127	2005-2021

[a] The altitude specifies the sampling height in meters above sea level. Stations considered as mountain sites are marked with an asterisk.

S2 Inversion ensembles

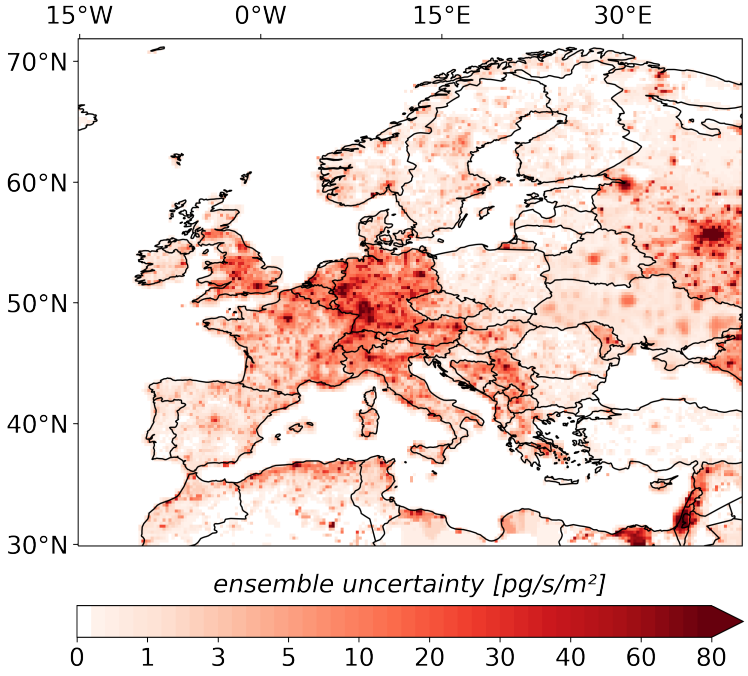

Figure S2. Ensemble uncertainty, presented as the range between the 92.5th–97.5th percentile range across all a posteriori emissions of the Monte Carlo ensemble at each grid cell

Table S3. Inversion settings generated using Monte Carlo methods. Parameters are sampled either continuously from a normal distribution within specified ranges or discretely from predefined values, as indicated in the table header. All inversions employ an emission grid configuration of 558 cells, and the baseline is optimized in 8 latitudinal bands with a temporal window of 30 days and a baseline uncertainty of 0.1 ppt.

Identifier	**A priori emission uncertainty** $\mathcal{N}(0.5, 0.1)$	**Minimum a priori emission uncertainty** $\mathcal{N}(5.e^{-13}, 1.e^{-13})$ [kgm^{-2}h^{-1}]	**Spatial correlation of the a priori emission uncertainty** $\mathcal{N}(250, 100)$ [km]	**Observation uncertainty** $\mathcal{N}(0.06, 0.01)$ [ppt]	**A priori emission inventories** all 7 inventories (see Sect. 2.3)	**Observation dataset** all 8 datasets (see Sect. 2.5)
0	0.41	6.9e-13	305	0.058	UN	Global: high-frequency surface stations
1	0.66	5.6e-13	89	0.052	E8	Global
2	0.48	4.6e-13	310	0.087	UP	Global: night/afternoon selection
3	0.52	3.5e-13	226	0.068	GAINS	Europe
4	0.49	5.4e-13	267	0.069	UN	Global: excluding mountain stations
5	0.53	6.1e-13	378	0.049	UN	Europe: high-frequency surface stations
6	0.61	4.9e-13	317	0.073	E7P	Europe: night/afternoon selection
7	0.42	4.8e-13	231	0.063	GAINS	Europe: excluding mountain stations
8	0.55	6.1e-13	50	0.056	E7P	Global: night/afternoon selection
9	0.42	4.4e-13	157	0.081	GS_HR	Europe: high-frequency surface stations
10	0.64	5.5e-13	316	0.042	E8	Global: excluding mountain stations
11	0.65	5.6e-13	455	0.069	UN	Europe: night/afternoon selection
12	0.43	4.0e-13	328	0.057	UP	Global: night/afternoon selection
13	0.61	7.1e-13	153	0.056	UP	Europe: night/afternoon selection
14	0.57	6.2e-13	161	0.068	GAINS	Global: night/afternoon selection
15	0.60	3.0e-13	320	0.048	GAINS	Europe
16	0.65	4.1e-13	377	0.069	E7P	Europe: excluding mountain stations
17	0.62	4.1e-13	309	0.062	E7N	Global: excluding mountain stations
18	0.52	4.7e-13	323	0.058	UP	Europe: night/afternoon selection
19	0.62	4.7e-13	267	0.060	E7N	Europe: high-frequency surface stations
20	0.47	5.3e-13	297	0.062	GAINS	Europe: high-frequency surface stations
21	0.52	6.9e-13	363	0.079	GAINS	Global
22	0.52	4.3e-13	352	0.072	GS_HR	Global: high-frequency surface stations
23	0.59	4.1e-13	275	0.069	E8	Global
24	0.36	4.7e-13	110	0.058	E7P	Global: excluding mountain stations
25	0.53	5.0e-13	274	0.056	E8	Global
26	0.51	5.3e-13	386	0.050	GS_HR	Europe: high-frequency surface stations
27	0.62	6.8e-13	65	0.067	E7P	Global: night/afternoon selection
28	0.67	3.4e-13	177	0.059	E8	Global: night/afternoon selection
29	0.42	6.2e-13	299	0.068	GAINS	Europe
30	0.64	7.7e-13	573	0.048	GS_HR	Europe: high-frequency surface stations
31	0.38	3.2e-13	378	0.075	UP	Europe: night/afternoon selection
32	0.41	4.5e-13	273	0.061	E8	Global
33	0.59	5.4e-13	409	0.053	UP	Global
34	0.72	5.2e-13	62	0.057	GS_HR	Europe: night/afternoon selection
35	0.54	2.8e-13	213	0.065	GAINS	Global: excluding mountain stations
36	0.52	5.6e-13	81	0.065	E7P	Europe: night/afternoon selection
37	0.33	5.2e-13	77	0.068	UN	Europe
38	0.51	5.8e-13	304	0.051	E8	Global: high-frequency surface stations
39	0.44	6.3e-13	85	0.075	UP	Europe: night/afternoon selection
40	0.39	4.8e-13	42	0.068	GS_HR	Europe: night/afternoon selection
41	0.30	4.1e-13	165	0.072	E7N	Europe: high-frequency surface stations
42	0.63	3.8e-13	130	0.058	UP	Global: night/afternoon selection
43	0.43	5.4e-13	285	0.046	UP	Global
44	0.45	3.8e-13	233	0.059	E7P	Europe: night/afternoon selection
45	0.61	3.7e-13	283	0.049	UP	Global: excluding mountain stations
46	0.42	5.3e-13	309	0.066	E7N	Global: high-frequency surface stations
47	0.52	4.4e-13	172	0.058	GAINS	Europe: night/afternoon selection
48	0.48	5.5e-13	191	0.058	UN	Global
49	0.51	3.0e-13	173	0.070	E7N	Europe: night/afternoon selection
50	0.53	4.0e-13	282	0.083	UN	Global: night/afternoon selection
51	0.57	4.2e-13	318	0.071	E8	Global: night/afternoon selection
52	0.52	4.4e-13	171	0.051	E7P	Global
53	0.52	6.0e-13	150	0.063	GAINS	Europe: high-frequency surface stations
54	0.50	5.6e-13	149	0.074	UP	Europe: excluding mountain stations
55	0.50	4.4e-13	327	0.054	E7P	Global: night/afternoon selection
56	0.50	6.2e-13	55	0.058	GAINS	Europe
57	0.53	5.0e-13	233	0.066	UP	Global: excluding mountain stations
58	0.41	4.6e-13	72	0.045	GS_HR	Global: high-frequency surface stations

Table S4. E59: Additional 59-member ensemble, generated using Monte Carlo methods. Parameters are sampled either continuously from a normal distribution within specified ranges or discretely from predefined values, as indicated in the table header. All inversions employ an emission grid configuration of 558 cells, and the baseline is optimized in 8 latitudinal bands with a temporal window of 30 days and a baseline uncertainty of 0.1 ppt.

Identifier	**A priori emission uncertainty** $\mathcal{N}(0.5, 0.1)$	**Minimum a priori emission uncertainty** $\mathcal{N}(5.e^{-13}, 1.e^{-13})$ [$kgm^{-2}h^{-1}$]	**Spatial correlation of the a priori emission uncertainty** $\mathcal{N}(250, 100)$ [km]	**Observation uncertainty** $\mathcal{N}(0.06, 0.01)$ [ppt]	**A priori emission inventories** all 7 inventories (see Sect. 2.3)	**Observation dataset** all 8 datasets (see Sect. 2.5)
0	0.49	4.8e-13	38	0.082	GAINS	Global: high-frequency surface stations
1	0.42	5.6e-13	241	0.050	UP	Global: night/afternoon selection
2	0.61	6.5e-13	207	0.055	UP	Europe
3	0.37	3.9e-13	167	0.068	GS_HR	Global
4	0.36	6.9e-13	235	0.037	E8	Europe: high-frequency surface stations
5	0.40	4.8e-13	141	0.050	GS_HR	Global: high-frequency surface stations
6	0.44	4.2e-13	100	0.049	GAINS	Europe
7	0.64	6.1e-13	34	0.064	GAINS	Europe
8	0.51	5.6e-13	228	0.049	E8	Europe: excluding mountain stations
9	0.45	6.9e-13	179	0.049	UN	Europe
10	0.43	5.3e-13	191	0.057	GAINS	Global: night/afternoon selection
11	0.55	6.5e-13	196	0.054	UN	Europe: excluding mountain stations
12	0.35	6.0e-13	179	0.068	UP	Europe: excluding mountain stations
13	0.39	4.6e-13	299	0.063	GAINS	Global: high-frequency surface stations
14	0.55	4.3e-13	330	0.080	GAINS	Global
15	0.44	6.5e-13	196	0.074	UP	Global: night/afternoon selection
16	0.65	4.6e-13	355	0.070	GAINS	Global
17	0.48	6.3e-13	147	0.045	UN	Global: high-frequency surface stations
18	0.42	5.2e-13	71	0.062	UN	Europe: night/afternoon selection
19	0.52	6.5e-13	199	0.060	UP	Global: high-frequency surface stations
20	0.36	5.8e-13	147	0.074	GS_HR	Global
21	0.41	4.7e-13	120	0.053	E7P	Global: night/afternoon selection
22	0.30	5.4e-13	297	0.066	E7P	Global: high-frequency surface stations
23	0.27	4.6e-13	186	0.063	UP	Europe: night/afternoon selection
24	0.67	5.6e-13	285	0.051	E8	Europe: night/afternoon selection
25	0.21	4.3e-13	130	0.063	UP	Global: high-frequency surface stations
26	0.51	5.6e-13	420	0.068	E7N	Europe
27	0.45	6.3e-13	398	0.043	GS_HR	Global: night/afternoon selection
28	0.49	4.9e-13	331	0.051	UN	Global: high-frequency surface stations
29	0.53	3.8e-13	285	0.058	E7P	Europe: high-frequency surface stations
30	0.73	5.4e-13	299	0.057	GS_HR	Europe
31	0.52	5.1e-13	190	0.058	UP	Global: excluding mountain stations
32	0.55	3.3e-13	178	0.068	UP	Europe: night/afternoon selection
33	0.43	4.8e-13	199	0.043	E8	Global: high-frequency surface stations
34	0.64	3.0e-13	344	0.064	GAINS	Global: night/afternoon selection
35	0.63	5.7e-13	310	0.076	E7P	Europe: excluding mountain stations
36	0.49	4.2e-13	185	0.059	E8	Global: night/afternoon selection
37	0.57	5.1e-13	66	0.054	UP	Europe: excluding mountain stations
38	0.67	5.3e-13	367	0.043	UP	Europe: night/afternoon selection
39	0.54	5.9e-13	253	0.056	E8	Global: high-frequency surface stations
40	0.46	4.4e-13	271	0.067	E8	Global: excluding mountain stations
41	0.52	5.6e-13	449	0.051	GS_HR	Europe: night/afternoon selection
42	0.59	6.6e-13	233	0.074	E8	Europe: night/afternoon selection
43	0.48	6.3e-13	376	0.034	E7N	Global: night/afternoon selection
44	0.56	6.0e-13	350	0.061	E7P	Europe: high-frequency surface stations
45	0.44	4.2e-13	273	0.061	E7N	Europe: night/afternoon selection
46	0.40	3.4e-13	143	0.042	GAINS	Global: excluding mountain stations
47	0.52	7.3e-13	331	0.073	GS_HR	Global: high-frequency surface stations
48	0.31	5.8e-13	291	0.054	E7P	Global: high-frequency surface stations
49	0.41	4.3e-13	450	0.071	GS_HR	Global: high-frequency surface stations
50	0.58	4.6e-13	130	0.053	GAINS	Europe: excluding mountain stations
51	0.44	4.4e-13	288	0.052	UN	Europe
52	0.53	3.9e-13	361	0.043	UP	Europe: excluding mountain stations
53	0.50	5.2e-13	335	0.052	GS_HR	Global: excluding mountain stations
54	0.68	6.1e-13	225	0.063	UN	Europe: night/afternoon selection
55	0.42	4.7e-13	381	0.062	E8	Europe
56	0.53	2.7e-13	75	0.058	GS_HR	Europe: excluding mountain stations
57	0.36	5.7e-13	195	0.060	GS_HR	Global: night/afternoon selection
58	0.51	4.2e-13	324	0.054	GAINS	Europe: night/afternoon selection

Table S5. E30: Additional 30-member ensemble, generated using Monte Carlo methods. Parameters are sampled either continuously from a normal distribution within specified ranges or discretely from predefined values, as indicated in the table header. All inversions employ an emission grid configuration of 558 cells, and the baseline is optimized in 8 latitudinal bands with a temporal window of 30 days and a baseline uncertainty of 0.1 ppt.

Identifier	**A priori emission uncertainty** $\mathcal{N}(0.5, 0.1)$	**Minimum a priori emission uncertainty** $\mathcal{N}(5.e^{-13}, 1.e^{-13})$ [kgm^{-2}h^{-1}]	**Spatial correlation of the a priori emission uncertainty** $\mathcal{N}(250, 100)$ [km]	**Observation uncertainty** $\mathcal{N}(0.06, 0.01)$ [ppt]	**A priori emission inventories** all 7 inventories (see Sect. 2.3)	**Observation dataset** all 8 datasets (see Sect. 2.5)
0	0.59	3.1e-13	310	0.060	E8	Global: high-frequency surface stations
1	0.44	7.1e-13	374	0.075	GAINS	Global: excluding mountain stations
2	0.48	5.5e-13	83	0.050	GAINS	Global: excluding mountain stations
3	0.53	3.2e-13	227	0.055	GAINS	Europe: high-frequency surface stations
4	0.51	4.0e-13	18	0.059	GS_HR	Global
5	0.38	4.5e-13	121	0.067	GS_HR	Europe: night/afternoon selection
6	0.50	5.8e-13	432	0.058	UN	Global: high-frequency surface stations
7	0.49	4.9e-13	191	0.052	GS_HR	Europe: night/afternoon selection
8	0.46	3.0e-13	224	0.057	GAINS	Europe
9	0.48	4.5e-13	178	0.055	E7P	Europe: night/afternoon selection
10	0.47	5.8e-13	26	0.051	E7N	Europe
11	0.57	3.5e-13	249	0.061	E7P	Europe: high-frequency surface stations
12	0.52	5.3e-13	284	0.063	UN	Europe: excluding mountain stations
13	0.61	5.0e-13	134	0.074	UN	Europe: excluding mountain stations
14	0.46	5.5e-13	327	0.046	E7P	Global
15	0.51	3.5e-13	386	0.072	E7N	Europe: excluding mountain stations
16	0.57	5.2e-13	232	0.058	E7P	Europe: high-frequency surface stations
17	0.38	5.7e-13	397	0.071	UN	Global: high-frequency surface stations
18	0.45	6.7e-13	334	0.061	UN	Global: high-frequency surface stations
19	0.52	5.8e-13	333	0.072	UP	Europe
20	0.62	4.8e-13	218	0.053	E8	Europe
21	0.49	4.7e-13	293	0.047	E8	Global: night/afternoon selection
22	0.36	4.4e-13	245	0.074	GS_HR	Europe: high-frequency surface stations
23	0.63	4.2e-13	368	0.055	UP	Global
24	0.55	7.2e-13	278	0.064	UN	Global: high-frequency surface stations
25	0.37	5.0e-13	317	0.076	E7P	Global: high-frequency surface stations
26	0.47	5.3e-13	295	0.065	E7N	Global
27	0.45	5.4e-13	159	0.051	UN	Europe: excluding mountain stations
28	0.49	5.5e-13	254	0.053	GAINS	Europe
29	0.54	5.4e-13	244	0.073	UP	Europe: excluding mountain stations

Table S6. E118: Additional 118-member ensemble, generated using Monte Carlo methods. Parameters are sampled either continuously from a normal distribution within specified ranges or discretely from predefined values, as indicated in the table header. All inversions employ an emission grid configuration of 558 cells, and the baseline is optimized in 8 latitudinal bands with a temporal window of 30 days and a baseline uncertainty of 0.1 ppt.

Identifier	**A priori emission uncertainty** $\mathcal{N}(0.5, 0.1)$	**Minimum a priori emission uncertainty** $\mathcal{N}(5.e^{-13}, 1.e^{-13})$ [$kgm^{-2}h^{-1}$]	**Spatial correlation of the a priori emission uncertainty** $\mathcal{N}(250, 100)$ [km]	**Observation uncertainty** $\mathcal{N}(0.06, 0.01)$ [ppt]	**A priori emission inventories** all 7 inventories (see Sect. 2.3)	**Observation dataset** all 8 datasets (see Sect. 2.5)
0	0.51	5.8e-13	178	0.064	E8	Global: night/afternoon selection
1	0.43	5.5e-13	242	0.045	UP	Global
2	0.32	5.1e-13	390	0.072	GAINS	Europe: high-frequency surface stations
3	0.53	5.5e-13	372	0.058	UP	Global: night/afternoon selection
4	0.37	5.4e-13	292	0.067	UN	Europe: high-frequency surface stations
5	0.55	6.8e-13	207	0.068	GS_HR	Global: night/afternoon selection
6	0.35	6.1e-13	161	0.056	GS_HR	Europe: high-frequency surface stations
7	0.68	6.2e-13	245	0.058	GS_HR	Global
8	0.45	4.7e-13	181	0.070	GS_HR	Europe: high-frequency surface stations
9	0.47	3.9e-13	277	0.073	UP	Europe
10	0.52	5.9e-13	216	0.046	E8	Global
11	0.67	4.6e-13	303	0.079	GS_HR	Europe: high-frequency surface stations
12	0.47	4.9e-13	151	0.057	GAINS	Global: excluding mountain stations
13	0.58	3.9e-13	309	0.064	GS_HR	Global: night/afternoon selection
14	0.53	5.6e-13	341	0.059	E7P	Global: night/afternoon selection
15	0.42	5.8e-13	464	0.070	E7P	Global: high-frequency surface stations
16	0.63	5.9e-13	247	0.056	UP	Europe: excluding mountain stations
17	0.65	4.6e-13	189	0.061	UP	Europe
18	0.42	5.4e-13	244	0.063	E7N	Europe
19	0.51	3.7e-13	388	0.028	E7P	Global: excluding mountain stations
20	0.41	3.4e-13	168	0.062	E8	Global: night/afternoon selection
21	0.50	3.6e-13	299	0.058	E7P	Europe
22	0.53	3.5e-13	283	0.057	UP	Europe: night/afternoon selection
23	0.52	4.3e-13	173	0.068	UP	Global: excluding mountain stations
24	0.40	5.5e-13	248	0.066	E7N	Global
25	0.55	3.8e-13	301	0.045	GS_HR	Europe: night/afternoon selection
26	0.62	3.2e-13	313	0.057	E7P	Europe
27	0.55	4.4e-13	241	0.064	E8	Global: high-frequency surface stations
28	0.45	5.6e-13	292	0.061	UN	Global: night/afternoon selection
29	0.44	4.9e-13	314	0.064	UN	Europe
30	0.49	4.9e-13	82	0.048	E8	Global: high-frequency surface stations
31	0.44	4.7e-13	247	0.052	E7P	Global: high-frequency surface stations
32	0.41	3.8e-13	342	0.047	GAINS	Global
33	0.39	6.1e-13	251	0.058	GS_HR	Global: high-frequency surface stations
34	0.72	5.4e-13	81	0.052	UN	Global: excluding mountain stations
35	0.49	5.5e-13	252	0.073	E8	Global: excluding mountain stations
36	0.27	5.3e-13	164	0.045	UP	Europe: night/afternoon selection
37	0.54	4.8e-13	318	0.058	E8	Europe: excluding mountain stations
38	0.58	4.3e-13	347	0.053	GAINS	Global: excluding mountain stations
39	0.56	4.4e-13	442	0.058	E7N	Global
40	0.54	5.4e-13	231	0.056	UP	Global: excluding mountain stations
41	0.56	4.0e-13	144	0.042	GAINS	Europe
42	0.54	4.7e-13	310	0.072	UP	Global
43	0.45	6.1e-13	243	0.064	GS_HR	Europe: excluding mountain stations
44	0.60	4.3e-13	286	0.066	E7P	Europe: high-frequency surface stations
45	0.42	3.6e-13	237	0.061	UP	Global: excluding mountain stations
46	0.34	4.8e-13	280	0.047	GAINS	Europe: high-frequency surface stations
47	0.46	4.5e-13	252	0.053	E7N	Europe: night/afternoon selection
48	0.54	4.2e-13	272	0.057	E8	Europe: excluding mountain stations
49	0.65	6.1e-13	375	0.064	GS_HR	Global: night/afternoon selection
50	0.63	5.3e-13	324	0.053	GAINS	Global: night/afternoon selection
51	0.45	5.3e-13	423	0.071	UP	Europe
52	0.66	3.4e-13	200	0.056	GAINS	Global
53	0.45	3.0e-13	410	0.047	GAINS	Europe
54	0.51	3.6e-13	266	0.061	E7N	Europe
55	0.61	5.1e-13	299	0.064	GS_HR	Europe: excluding mountain stations
56	0.45	4.8e-13	178	0.054	UN	Europe: excluding mountain stations
57	0.61	5.8e-13	281	0.073	GS_HR	Global: excluding mountain stations
58	0.56	4.3e-13	85	0.051	E7P	Europe

Identifier	**A priori emission uncertainty** $\mathcal{N}(0.5, 0.1)$	**Minimum a priori emission uncertainty** $\mathcal{N}(5.e^{-13}, 1.e^{-13})$ [kgm^{-2}h^{-1}]	**Spatial correlation of the a priori emission uncertainty** $\mathcal{N}(250, 100)$ [km]	**Observation uncertainty** $\mathcal{N}(0.06, 0.01)$ [ppt]	**A priori emission inventories** all 7 inventories (see Sect. 2.3)	**Observation dataset** all 8 datasets (see Sect. 2.5)
59	0.64	4.5e-13	362	0.073	E7P	Global
60	0.36	4.1e-13	168	0.048	E8	Global
61	0.54	5.0e-13	266	0.063	E7N	Europe: excluding mountain stations
62	0.20	6.8e-13	34	0.062	UN	Europe: excluding mountain stations
63	0.63	2.8e-13	282	0.072	GAINS	Europe: night/afternoon selection
64	0.46	3.8e-13	271	0.059	UP	Global: night/afternoon selection
65	0.41	3.8e-13	180	0.051	UP	Global
66	0.59	5.5e-13	87	0.064	E8	Global: excluding mountain stations
67	0.48	5.8e-13	57	0.054	GS_HR	Europe
68	0.48	3.7e-13	231	0.047	E7N	Global: night/afternoon selection
69	0.58	4.4e-13	285	0.062	UN	Global: night/afternoon selection
70	0.51	4.1e-13	257	0.059	UP	Europe: night/afternoon selection
71	0.55	3.3e-13	349	0.065	E7N	Global: high-frequency surface stations
72	0.43	5.2e-13	259	0.078	E7N	Global: excluding mountain stations
73	0.51	5.7e-13	408	0.060	E7N	Global: night/afternoon selection
74	0.57	3.2e-13	352	0.065	GAINS	Europe: night/afternoon selection
75	0.52	6.3e-13	422	0.058	E8	Global: excluding mountain stations
76	0.60	5.2e-13	293	0.068	GAINS	Global: excluding mountain stations
77	0.58	4.9e-13	140	0.062	E8	Global: high-frequency surface stations
78	0.40	4.1e-13	291	0.062	UN	Europe: high-frequency surface stations
79	0.42	4.2e-13	77	0.065	UP	Global
80	0.76	6.8e-13	312	0.057	GS_HR	Global: high-frequency surface stations
81	0.37	4.8e-13	157	0.066	GS_HR	Global: high-frequency surface stations
82	0.24	5.6e-13	223	0.058	E7N	Europe: high-frequency surface stations
83	0.60	4.6e-13	204	0.064	E7P	Europe
84	0.61	5.7e-13	159	0.058	GAINS	Europe: night/afternoon selection
85	0.49	4.4e-13	268	0.056	E7P	Global: high-frequency surface stations
86	0.47	5.5e-13	377	0.073	UP	Europe: excluding mountain stations
87	0.41	5.8e-13	281	0.075	UN	Europe: night/afternoon selection
88	0.34	5.8e-13	156	0.073	E7P	Global: high-frequency surface stations
89	0.46	6.7e-13	196	0.051	E7P	Global
90	0.61	3.4e-13	295	0.052	GS_HR	Global: high-frequency surface stations
91	0.35	5.1e-13	229	0.055	E7N	Global: high-frequency surface stations
92	0.46	4.2e-13	153	0.046	UP	Global: high-frequency surface stations
93	0.18	5.1e-13	226	0.054	UP	Global: excluding mountain stations
94	0.44	4.0e-13	254	0.058	E7P	Europe: high-frequency surface stations
95	0.45	5.9e-13	184	0.069	GS_HR	Global: high-frequency surface stations
96	0.54	4.3e-13	261	0.075	GAINS	Europe: high-frequency surface stations
97	0.51	6.9e-13	284	0.067	E7N	Global
98	0.62	6.3e-13	394	0.072	E8	Europe: excluding mountain stations
99	0.69	4.7e-13	285	0.074	E7N	Europe
100	0.53	5.5e-13	157	0.066	GAINS	Europe: high-frequency surface stations
101	0.35	4.5e-13	141	0.074	UP	Global
102	0.45	4.5e-13	271	0.078	UN	Europe: night/afternoon selection
103	0.32	5.0e-13	139	0.077	UN	Europe: excluding mountain stations
104	0.60	5.5e-13	174	0.070	GS_HR	Europe: excluding mountain stations
105	0.35	6.8e-13	203	0.062	GS_HR	Global: night/afternoon selection
106	0.51	6.1e-13	128	0.054	E8	Global: high-frequency surface stations
107	0.54	3.9e-13	329	0.055	GS_HR	Global: excluding mountain stations
108	0.55	4.0e-13	292	0.062	UN	Europe: high-frequency surface stations
109	0.55	4.6e-13	148	0.050	GAINS	Global: excluding mountain stations
110	0.53	3.6e-13	251	0.075	GS_HR	Global: excluding mountain stations
111	0.53	4.9e-13	223	0.074	GS_HR	Global: night/afternoon selection
112	0.53	5.2e-13	149	0.066	UP	Europe: night/afternoon selection
113	0.30	4.4e-13	364	0.054	GS_HR	Europe: high-frequency surface stations
114	0.50	5.8e-13	308	0.061	UP	Global: night/afternoon selection
115	0.53	4.7e-13	291	0.056	E7P	Europe: excluding mountain stations
116	0.46	5.2e-13	251	0.053	E7P	Global: excluding mountain stations
117	0.34	6.0e-13	137	0.066	E8	Europe

S3 Evaluation of model performance

We show the model–measurement agreement in Tab. S7 (r, RMSE, and bias) and with a Taylor diagram (Fig. S3). The Taylor diagram summarizes the match between observed and simulated values by showing: (i) the Pearson correlation coefficient (r), represented by the azimuthal angle, and (ii) the normalized standard deviation, represented by the radial distance from the origin. Each colored arrow represents a station, where the tail represents the a priori and the head the a posteriori simulated mole fractions. The length of each arrow represents the difference between the a priori and a posteriori modeled mole fractions with respect to the observed mixing ratios, indicating the correction made by the inversion.

Overall, the Taylor diagram highlights the most pronounced statistical improvements at the UK stations TAC, HFD, RGL, and BSD. The Pearson correlation coefficient increased by about 0.1 at TAC and HFD, and by around 0.05 at RGL and BSD, averaged over their respective operating years. These stations also show substantial reductions in both bias and RMSE (see Tab. S7). The Taylor plot further shows notable improvements at ZEP, MHD, and the mountain station ZSF in individual years. The other European mountain stations, JFJ and CMN, also exhibit modest increases in r values (around 0.02) but pronounced reductions in bias. Finally, Fig. S3 clearly differentiates between stations inside and outside Europe, with non-European stations showing little to no improvement in r values. However, some display reductions in bias and RMSE, most likely due to the improved baseline (Tab. S7).

Table S7. Model–measurement agreement (r, RMSE, and bias) before and after the inversion using the reference setting. Values are shown for individual stations and averaged over the study period.

Station	Correlation (r) (a priori)	Correlation (r) (a posteriori)	RMSE (a priori) [ppt]	RMSE (a posteriori) [ppt]	Bias (a priori) [ppt]	Bias (a posteriori) [ppt]
BIK	0.795	0.774	0.080	0.081	-0.024	0.024
BRM	0.301	0.411	0.245	0.219	-0.104	-0.070
BRW	0.815	0.820	0.071	0.061	-0.029	0.003
BSD	0.848	0.887	0.080	0.063	-0.028	0.004
CGO	0.964	0.960	0.033	0.029	0.006	0.006
CMN	0.479	0.477	0.207	0.180	-0.122	-0.048
COI	0.456	0.473	0.146	0.135	-0.054	-0.005
GSN	0.408	0.411	0.800	0.779	-0.380	-0.339
HAT	0.593	0.592	0.302	0.291	-0.075	-0.031
HFD	0.735	0.829	0.118	0.096	0.002	0.024
IZO	0.810	0.807	0.072	0.069	-0.030	0.020
JFJ	0.703	0.722	0.123	0.110	-0.055	-0.009
MHD	0.883	0.904	0.060	0.046	-0.032	0.005
MLO	0.704	0.708	0.101	0.120	0.035	0.074
NWR	0.687	0.690	0.121	0.100	-0.068	-0.024
RGL	0.804	0.855	0.102	0.072	-0.059	-0.011
RPB	0.911	0.904	0.046	0.052	-0.012	0.025
SMO	0.837	0.819	0.056	0.057	0.001	0.011
SPO	0.871	0.871	0.054	0.053	0.000	-0.000
SUM	0.795	0.797	0.077	0.064	-0.039	0.001
TAC	0.718	0.817	0.133	0.100	-0.050	-0.005
THD	0.842	0.858	0.071	0.054	-0.043	-0.005
ZEP	0.869	0.870	0.054	0.048	-0.023	0.010
ZSF	0.654	0.717	0.118	0.099	-0.027	-0.005
Mean	0.728	0.749	0.136	0.124	-0.050	-0.014

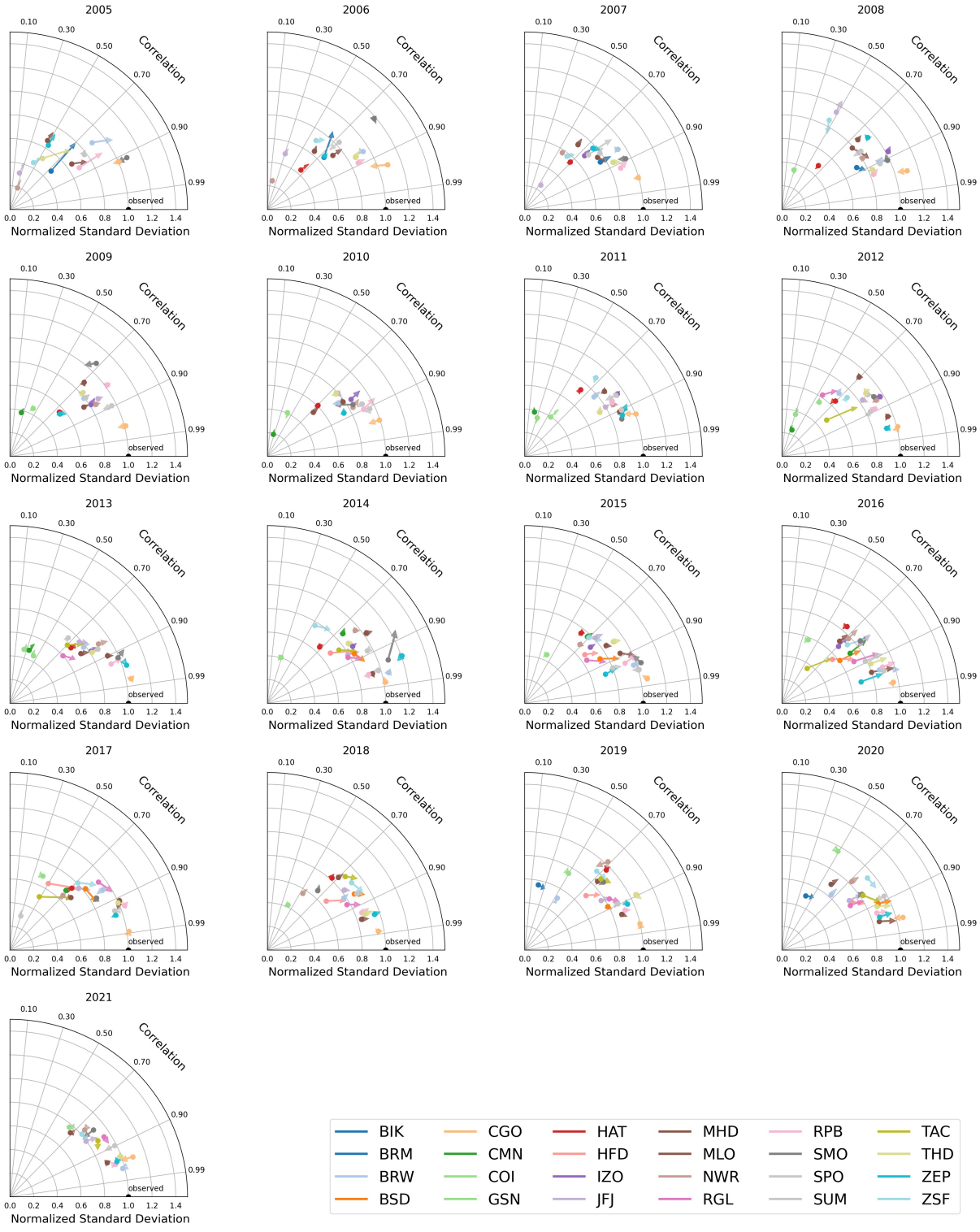

Figure S3. Taylor diagrams for comparing the *a priori* and *a posteriori* simulated mole fractions to the observed mixing ratios at all continuous stations, for the years 2005-2021.

S4 National emissions

Table S8. A posteriori emission values for the United Kingdom, Germany, France, Italy, and the EU-27 for the period 2005 to 2021. The values present the average over the entire Monte Carlo inversion ensemble with a 2.5th–97.5th percentile uncertainty range.

year	United Kingdom [t yr^{-1}]	Germany [t yr^{-1}]	France [t yr^{-1}]	Italy [t yr^{-1}]	EU-27 [t yr^{-1}]
2005	38 (31-46)	182 (155-251)	78 (51-117)	33 (26-46)	403 (335-501)
2006	55 (45-63)	182 (161-209)	59 (39-92)	28 (17-44)	344 (288-422)
2007	44 (29-62)	164 (133-188)	45 (20-80)	28 (14-46)	323 (270-402)
2008	68 (47-77)	98 (68-162)	90 (53-138)	36 (24-55)	296 (218-435)
2009	41 (27-55)	136 (116-152)	46 (27-63)	39 (22-59)	303 (251-364)
2010	38 (26-49)	117 (103-135)	51 (33-75)	46 (23-67)	305 (253-359)
2011	38 (24-62)	102 (78-134)	46 (31-65)	34 (24-45)	259 (221-296)
2012	49 (42-59)	117 (98-144)	72 (41-97)	48 (24-76)	321 (272-387)
2013	31 (23-40)	86 (66-109)	77 (48-96)	45 (26-64)	285 (229-355)
2014	33 (26-39)	144 (131-155)	65 (39-83)	28 (19-36)	315 (277-355)
2015	29 (23-33)	138 (125-149)	54 (36-73)	43 (25-66)	302 (264-347)
2016	32 (27-37)	152 (134-191)	82 (49-108)	38 (20-79)	349 (287-438)
2017	26 (21-30)	199 (172-241)	55 (34-75)	39 (21-61)	396 (311-490)
2018	19 (15-26)	109 (97-125)	47 (30-62)	33 (19-49)	256 (216-303)
2019	18 (14-25)	119 (110-128)	46 (26-63)	32 (15-58)	270 (230-319)
2020	18 (13-24)	119 (107-144)	50 (30-64)	25 (12-47)	300 (235-366)
2021	19 (15-26)	97 (88-104)	35 (19-54)	27 (10-54)	225 (191-260)

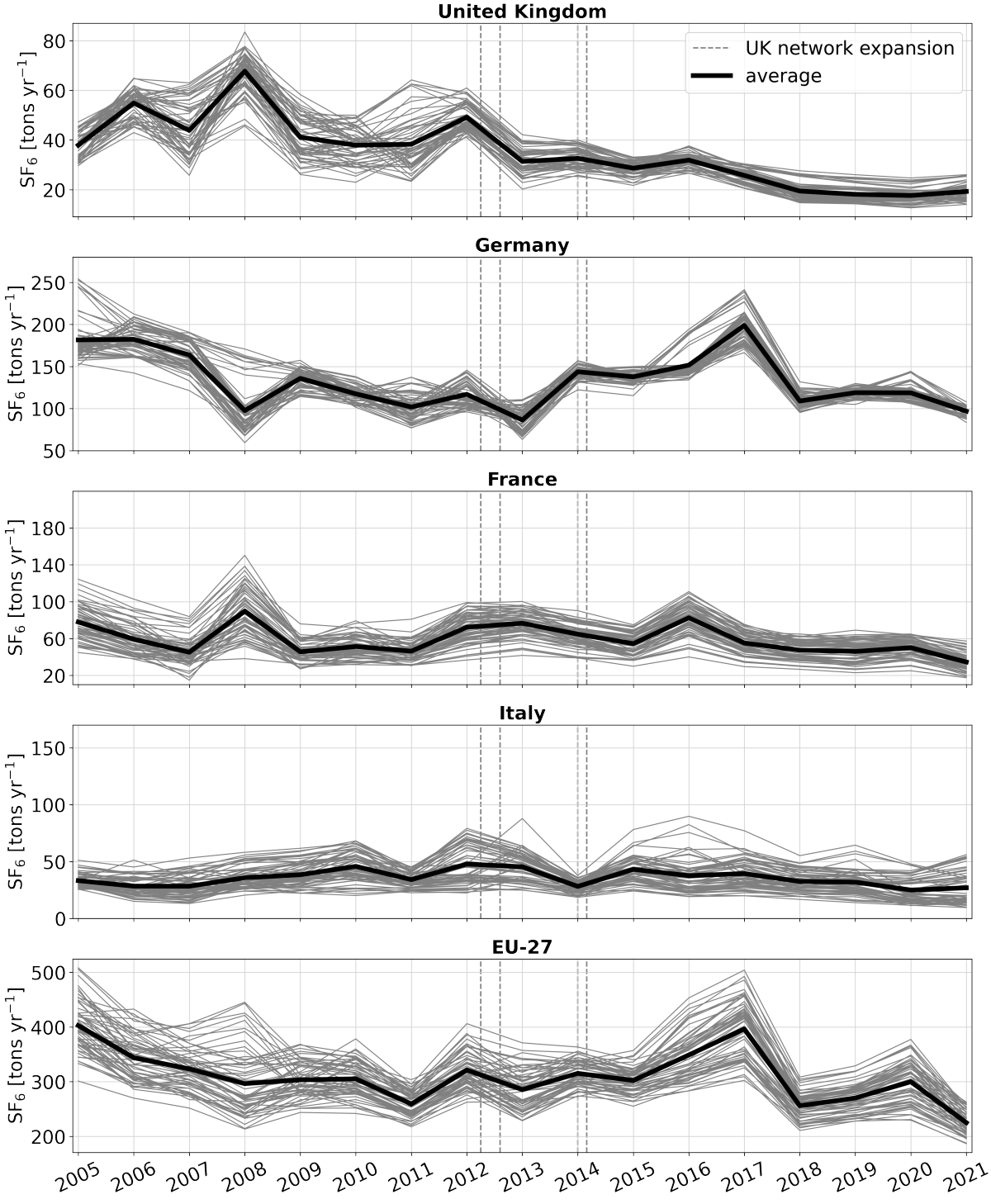

Figure S4. Annual emission time series for (a) the United Kingdom, (b) Germany, (c) France, (d) Italy, and (e) the EU-27. The solid gray lines represent all inversion results using the Monte Carlo-based settings. The solid black lines represent the average a posteriori emissions across all performed inversions,

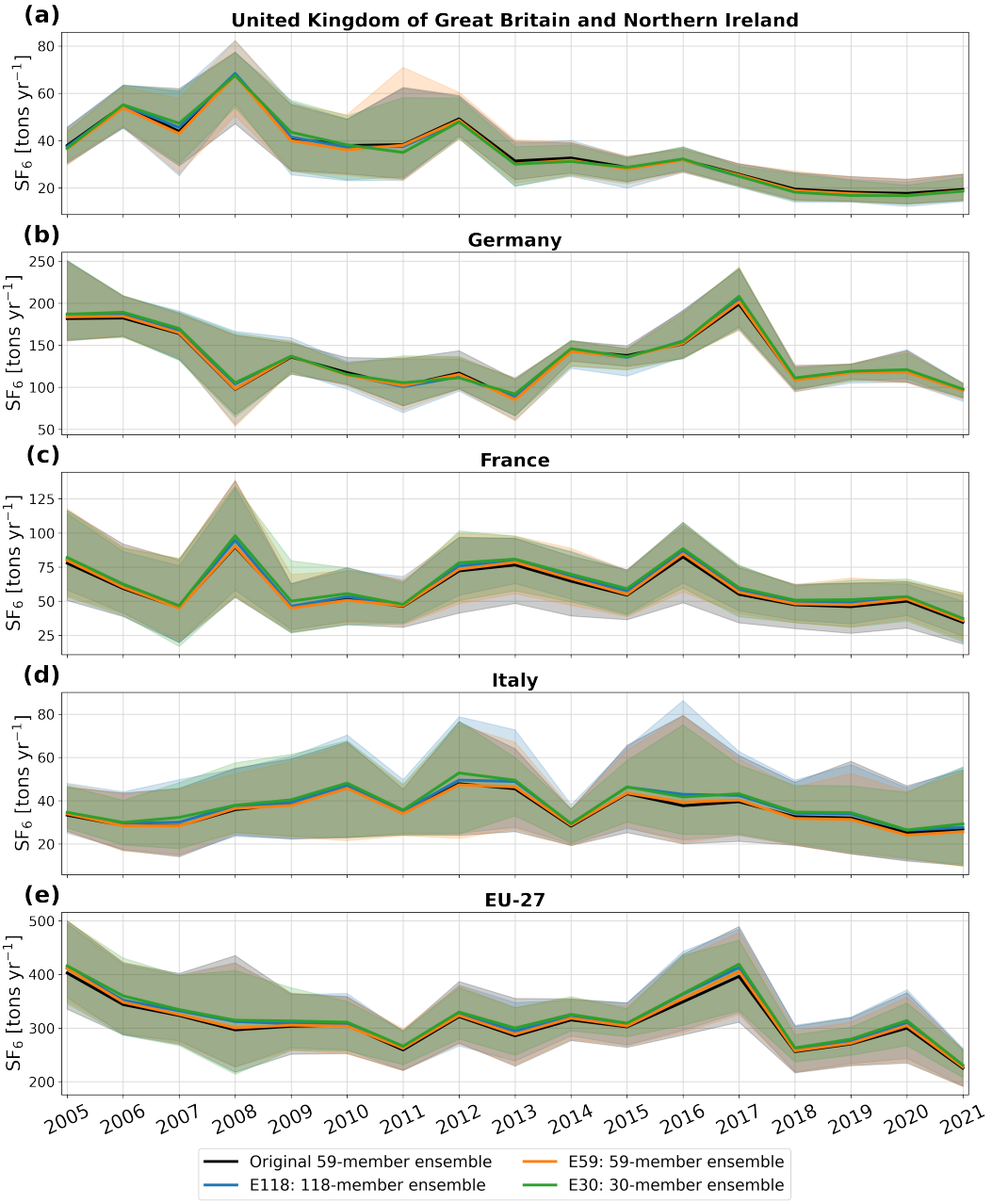

Figure S5. Comparison of the original 59-member Monte Carlo ensemble (black) with three additional ensembles: E30 (30 members), E59 (59 members), and E118 (118 members). Panels show annual a posteriori emission time series for (a) the United Kingdom, (b) Germany, (c) France, (d) Italy, and (e) the EU-27. Solid lines denote the ensemble mean, and shaded areas indicate the 2.5th–97.5th percentile range for each year.

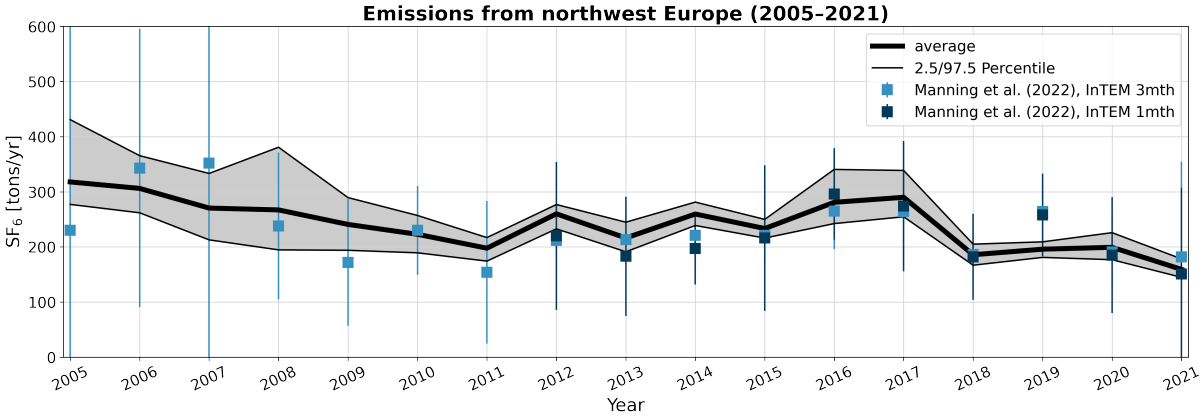

Figure S6. Annual emission time series for northwest Europe. The solid black lines represent the average a posteriori emissions across all performed inversions, and shaded areas indicate the 2.5th–97.5th percentile range for each year. The blue and black squares represent the results from Manning et al. (2022) using the InTEM model with inversion time frames set to 3- and 1-months, respectively

S5 Sensitivity test statistics

Table S9. Model–measurement agreement (r, RMSE, and bias) before and after the inversion using a spatial a priori correlation length of 500 km. Values are shown for individual stations and averaged over the study period.

Station	Correlation (r) (a priori)	Correlation (r) (a posteriori)	RMSE (a priori) [ppt]	RMSE (a posteriori) [ppt]	Bias (a priori) [ppt]	Bias (a posteriori) [ppt]
BIK	0.795	0.754	0.080	0.087	-0.024	0.028
BRM	0.301	0.399	0.245	0.221	-0.104	-0.070
BRW	0.815	0.817	0.071	0.063	-0.029	0.002
BSD	0.848	0.884	0.080	0.064	-0.028	0.005
CGO	0.964	0.960	0.033	0.045	0.006	0.031
CMN	0.479	0.472	0.207	0.180	-0.122	-0.048
COI	0.456	0.454	0.146	0.136	-0.054	-0.013
GSN	0.408	0.411	0.800	0.783	-0.380	-0.347
HAT	0.593	0.594	0.302	0.294	-0.075	-0.041
HFD	0.735	0.825	0.118	0.098	0.002	0.028
IZO	0.810	0.810	0.072	0.065	-0.030	0.007
JFJ	0.703	0.719	0.123	0.111	-0.055	-0.012
MHD	0.883	0.902	0.060	0.046	-0.032	0.004
MLO	0.704	0.708	0.101	0.113	0.035	0.063
NWR	0.687	0.686	0.121	0.105	-0.068	-0.038
RGL	0.804	0.851	0.102	0.073	-0.059	-0.011
RPB	0.911	0.910	0.046	0.047	-0.012	0.017
SMO	0.837	0.833	0.056	0.065	0.001	0.027
SPO	0.871	0.869	0.054	0.060	0.000	0.025
SUM	0.795	0.793	0.077	0.065	-0.039	-0.001
TAC	0.718	0.813	0.133	0.101	-0.050	-0.004
THD	0.842	0.853	0.071	0.055	-0.043	-0.013
ZEP	0.869	0.869	0.054	0.049	-0.023	0.011
ZSF	0.654	0.705	0.118	0.101	-0.027	-0.007
Mean	0.728	0.745	0.136	0.126	-0.050	-0.015

Table S10. Model–measurement agreement (r, RMSE, and bias) before and after the inversion using a spatial a priori correlation length of 1000 km. Values are shown for individual stations and averaged over the study period.

Station	Correlation (r) (a priori)	Correlation (r) (a posteriori)	RMSE (a priori) [ppt]	RMSE (a posteriori) [ppt]	Bias (a priori) [ppt]	Bias (a posteriori) [ppt]
BIK	0.795	0.743	0.080	0.089	-0.024	0.031
BRM	0.301	0.387	0.245	0.223	-0.104	-0.071
BRW	0.815	0.817	0.071	0.063	-0.029	0.002
BSD	0.848	0.883	0.080	0.064	-0.028	0.005
CGO	0.964	0.960	0.033	0.045	0.006	0.031
CMN	0.479	0.468	0.207	0.181	-0.122	-0.050
COI	0.456	0.453	0.146	0.136	-0.054	-0.013
GSN	0.408	0.411	0.800	0.783	-0.380	-0.347
HAT	0.593	0.594	0.302	0.294	-0.075	-0.041
HFD	0.735	0.819	0.118	0.101	0.002	0.030
IZO	0.810	0.810	0.072	0.065	-0.030	0.008
JFJ	0.703	0.717	0.123	0.112	-0.055	-0.011
MHD	0.883	0.901	0.060	0.046	-0.032	0.004
MLO	0.704	0.708	0.101	0.113	0.035	0.063
NWR	0.687	0.686	0.121	0.105	-0.068	-0.038
RGL	0.804	0.848	0.102	0.074	-0.059	-0.012
RPB	0.911	0.910	0.046	0.047	-0.012	0.017
SMO	0.837	0.833	0.056	0.065	0.001	0.026
SPO	0.871	0.869	0.054	0.060	0.000	0.025
SUM	0.795	0.793	0.077	0.065	-0.039	-0.001
TAC	0.718	0.807	0.133	0.102	-0.050	-0.006
THD	0.842	0.852	0.071	0.055	-0.043	-0.013
ZEP	0.869	0.869	0.054	0.049	-0.023	0.011
ZSF	0.654	0.701	0.118	0.102	-0.027	-0.007
Mean	0.728	0.743	0.136	0.127	-0.050	-0.015

Table S11. Model–measurement agreement (r, RMSE, and bias) before and after the inversion using a baseline uncertainty of 0.0001 ppt. Values are shown for individual stations and averaged over the study period.

Station	Correlation (r) (a priori)	Correlation (r) (a posteriori)	RMSE (a priori) [ppt]	RMSE (a posteriori) [ppt]	Bias (a priori) [ppt]	Bias (a posteriori) [ppt]
BIK	0.795	0.756	0.080	0.086	-0.024	0.026
BRM	0.301	0.388	0.245	0.223	-0.104	-0.070
BRW	0.815	0.817	0.071	0.064	-0.029	-0.012
BSD	0.848	0.879	0.080	0.065	-0.028	0.000
CGO	0.964	0.964	0.033	0.033	0.006	0.007
CMN	0.479	0.474	0.207	0.182	-0.122	-0.053
COI	0.456	0.447	0.146	0.139	-0.054	-0.022
GSN	0.408	0.408	0.800	0.791	-0.380	-0.363
HAT	0.593	0.590	0.302	0.298	-0.075	-0.063
HFD	0.735	0.831	0.118	0.096	0.002	0.021
IZO	0.810	0.804	0.072	0.067	-0.030	-0.013
JFJ	0.703	0.711	0.123	0.113	-0.055	-0.020
MHD	0.883	0.898	0.060	0.048	-0.032	-0.007
MLO	0.704	0.702	0.101	0.104	0.035	0.044
NWR	0.687	0.687	0.121	0.115	-0.068	-0.058
RGL	0.804	0.848	0.102	0.075	-0.059	-0.016
RPB	0.911	0.909	0.046	0.044	-0.012	-0.003
SMO	0.837	0.837	0.056	0.056	0.001	0.003
SPO	0.871	0.871	0.054	0.054	0.000	0.001
SUM	0.795	0.789	0.077	0.068	-0.039	-0.018
TAC	0.718	0.811	0.133	0.102	-0.050	-0.010
THD	0.842	0.840	0.071	0.063	-0.043	-0.030
ZEP	0.869	0.859	0.054	0.050	-0.023	-0.001
ZSF	0.654	0.698	0.118	0.104	-0.027	-0.011
Mean	0.728	0.742	0.136	0.127	-0.050	-0.028

Table S12. Model–measurement agreement (r, RMSE, and bias) before and after the inversion using a baseline uncertainty of 0.001 ppt. Values are shown for individual stations and averaged over the study period.

Station	Correlation (r) (a priori)	Correlation (r) (a posteriori)	RMSE (a priori) [ppt]	RMSE (a posteriori) [ppt]	Bias (a priori) [ppt]	Bias (a posteriori) [ppt]
BIK	0.795	0.773	0.080	0.081	-0.024	0.025
BRM	0.301	0.408	0.245	0.220	-0.104	-0.070
BRW	0.815	0.820	0.071	0.062	-0.029	0.006
BSD	0.848	0.887	0.080	0.063	-0.028	0.005
CGO	0.964	0.962	0.033	0.029	0.006	0.009
CMN	0.479	0.479	0.207	0.180	-0.122	-0.049
COI	0.456	0.464	0.146	0.136	-0.054	-0.006
GSN	0.408	0.411	0.800	0.781	-0.380	-0.343
HAT	0.593	0.592	0.302	0.293	-0.075	-0.038
HFD	0.735	0.829	0.118	0.097	0.002	0.025
IZO	0.810	0.809	0.072	0.066	-0.030	0.013
JFJ	0.703	0.723	0.123	0.110	-0.055	-0.011
MHD	0.883	0.904	0.060	0.046	-0.032	0.006
MLO	0.704	0.707	0.101	0.116	0.035	0.068
NWR	0.687	0.689	0.121	0.102	-0.068	-0.032
RGL	0.804	0.854	0.102	0.072	-0.059	-0.010
RPB	0.911	0.908	0.046	0.048	-0.012	0.020
SMO	0.837	0.833	0.056	0.057	0.001	0.014
SPO	0.871	0.871	0.054	0.053	0.000	0.001
SUM	0.795	0.795	0.077	0.065	-0.039	0.003
TAC	0.718	0.817	0.133	0.100	-0.050	-0.004
THD	0.842	0.854	0.071	0.055	-0.043	-0.008
ZEP	0.869	0.872	0.054	0.049	-0.023	0.013
ZSF	0.654	0.713	0.118	0.100	-0.027	-0.006
Mean	0.728	0.749	0.136	0.124	-0.050	-0.015

Table S13. Model–measurement agreement (r, RMSE, and bias) before and after the inversion using a baseline uncertainty of 0.01 ppt. Values are shown for individual stations and averaged over the study period.

Station	Correlation (r) (a priori)	Correlation (r) (a posteriori)	RMSE (a priori) [ppt]	RMSE (a posteriori) [ppt]	Bias (a priori) [ppt]	Bias (a posteriori) [ppt]
BIK	0.795	0.774	0.080	0.081	-0.024	0.024
BRM	0.301	0.411	0.245	0.219	-0.104	-0.070
BRW	0.815	0.820	0.071	0.061	-0.029	0.003
BSD	0.848	0.887	0.080	0.063	-0.028	0.004
CGO	0.964	0.960	0.033	0.029	0.006	0.006
CMN	0.479	0.477	0.207	0.180	-0.122	-0.048
COI	0.456	0.472	0.146	0.135	-0.054	-0.005
GSN	0.408	0.411	0.800	0.779	-0.380	-0.339
HAT	0.593	0.591	0.302	0.291	-0.075	-0.031
HFD	0.735	0.829	0.118	0.096	0.002	0.024
IZO	0.810	0.807	0.072	0.068	-0.030	0.020
JFJ	0.703	0.722	0.123	0.110	-0.055	-0.009
MHD	0.883	0.904	0.060	0.046	-0.032	0.005
MLO	0.704	0.708	0.101	0.120	0.035	0.073
NWR	0.687	0.690	0.121	0.100	-0.068	-0.025
RGL	0.804	0.855	0.102	0.072	-0.059	-0.011
RPB	0.911	0.905	0.046	0.052	-0.012	0.025
SMO	0.837	0.820	0.056	0.057	0.001	0.011
SPO	0.871	0.871	0.054	0.053	0.000	-0.001
SUM	0.795	0.797	0.077	0.064	-0.039	0.002
TAC	0.718	0.817	0.133	0.100	-0.050	-0.005
THD	0.842	0.858	0.071	0.054	-0.043	-0.005
ZEP	0.869	0.870	0.054	0.048	-0.023	0.010
ZSF	0.654	0.716	0.118	0.099	-0.027	-0.005
Mean	0.728	0.749	0.136	0.124	-0.050	-0.014

References

Manning, A., Redington, A., O'Doherty, S., Say, D., Young, D., Arnold, T., Rennick, C., Rigby, M., Wisher, A., and Simmonds, P.: Long-Term Atmospheric Measurement and Interpretation of Radiatively Active Trace Gases–Detailed Report (September 2019 to August 2020), Tech. rep., Department for Business, Energy & Industrial Strategy, https://assets.publishing.service.gov.uk/media/62d7b9bee90e071e7e59c97e/verification-uk-greenhouse-gas-emissions-using-atmospheric-observations-annual-report-2021.pdf, (last access 10 November 2023), 2022.